A Method for Spatially Resolved Local Intracellular Mechanochemical Sensing and Organelle Manipulation

S. Shekhar,[†] A. Cambi,[†‡] C. G. Figdor,[‡] V. Subramaniam,[†] and J. S. Kanger[†*]
[†]Department of Nanobiophysics, MIRA Institute for Biomedical Technology and Technical Medicine, University of Twente, Enschede, The Netherlands; and [‡]Department of Tumor Immunology, Nijmegen Centre for Molecular Life Sciences, Radboud University, Nijmegen, The Netherlands

ABSTRACT Because both the chemical and mechanical properties of living cells play crucial functional roles, there is a strong need for biophysical methods to address these properties simultaneously. Here we present a novel (to our knowledge) approach to measure local intracellular micromechanical and chemical properties using a hybrid magnetic chemical biosensor. We coupled a fluorescent dye, which serves as a chemical sensor, to a magnetic particle that is used for measurement of the viscoelastic environment by studying the response of the particle to magnetic force pulses. As a demonstration of the potential of this approach, we applied the method to study the process of phagocytosis, wherein cytoskeletal reorganization occurs in parallel with acidification of the phagosome. During this process, we measured the shear modulus and viscosity of the phagosomal environment concurrently with the phagosomal pH. We found that it is possible to manipulate phagocytosis by stalling the centripetal movement of the phagosome using magnetic force. Our results suggest that preventing centripetal phagosomal transport delays the onset of acidification. To our knowledge, this is the first report of manipulation of intracellular phagosomal transport without interfering with the underlying motor proteins or cytoskeletal network through biochemical methods.

INTRODUCTION

Cells act in response to changes in their immediate and extended (bio-)chemical and physical environment. This includes changes in the concentrations of chemical species, temperature, and substrate properties, among other factors (1). Cells respond to these changes in a variety of ways, such as by turning on the expression of a protein/enzyme or by orienting themselves in a voltage gradient (2,3). Traditionally, cellular processes have been studied in the light of changes in concentrations of various biochemical species. Most such changes, especially those related to cell movement or morphology, are often accompanied by a reorganization of the cellular cytoskeleton, which leads to changes in the mechanical properties of cells. There is an increasing recognition of the role played by mechanobiology in these processes. Intracellular micromechanical properties, such as cell stiffness, have been shown to play an important role in various diseases, including cancer. Tumor cells exhibit altered micromechanical properties as the tumor progresses (2). Chemical and mechanical properties are intimately interlinked, i.e., changes in chemical concentrations can lead to changes in micromechanical properties and vice versa. Intracellular chemical and mechanical properties have largely been measured separately. To gain a better understanding of their interdependence, it is essential to devise tools that allow simultaneous micromechanical and chemical measurements of the intracellular environment. We previously reported a novel biophysical method that allowed spatially resolved chemical sensing with the use of functionalized magnetic probes. In this work, we report on recent developments that exploit the magnetic properties of the probe to include both microrheology measurements and chemical sensing. The method is based on a combination of magnetic tweezers and fluorescent microscopy.

The study of cellular mechanical properties is referred to as microrheology. There are two types of microrheology: active and passive (3). Active microrheology involves inferring viscoelastic properties from deformations caused by an external applied force, whereas passive microrheology involves tracking the motion of intracellular tracer particles caused by Brownian fluctuations. The viscoelastic properties measured by these methods largely depend on the appropriate theoretical models and on the coupling between tracers and the cell, and can therefore lead to measurement of artifacts. In addition, the accuracy of passive microrheology can be limited by non-Brownian tracer motions such as motor trafficking, cytoskeleton remodeling, and cell locomotion. Therefore, the validity of these methods has been a topic of some debate (3).

In earlier studies, tools such as atomic force microscopy (AFM) (4), micropipettes (5), and optical tweezers (6) were employed for microrheology measurements. AFM has been used to extract mechanical properties by measuring the interaction of the cantilever with the plasma membrane; however, its application has been limited to whole-cell measurements and to regions close to the plasma membrane. Optical tweezers suffer from their inability to apply high intracellular forces and their lack of specificity in trapping probes in an intracellular environment composed of a myriad of refractive indices. Magnetic tweezers have successfully eliminated these limitations because applied forces are

Submitted February 6, 2012, and accepted for publication June 4, 2012.

*Correspondence: j.s.kanger@utwente.nl

Editor: George Barisas.

0006-3495/12/08/0395/10 $2.00

http://dx.doi.org/10.1016/j.bpj.2012.06.010

very specific to magnetic particles, and hence they minimally affect normal cellular processes and structures. Compared with optical tweezers, magnetic tweezers can also exert much higher forces (approximately nanonewtons). Magnetic tweezers have been used for microrheology in two different ways. The first involves letting a magnetic particle align along an applied magnetic field and measuring the particle relaxation when the field is switched off (7). The second, more commonly applied technique involves applying a linear force on a magnetic probe by a magnetic field gradient. Displacement of the probe in response to the force provides a measure of the mechanical properties of the probe environment. This method has been extensively used to measure the micromechanical properties of both the cytoplasm and the cell nucleus (8,9). In this work, we used magnetic particles in combination with magnetic tweezers, an approach that allows us to carry out passive and active microrheology studies simultaneously using a single tracer particle. An additional advantage is that this method allows a direct comparison of the two microrheology approaches.

Here, we present a novel (to our knowledge) approach for obtaining intracellular chemical sensing and micromechanical measurements simultaneously using a single probe. This approach is based on functionalizing a magnetic particle with a fluorescent dye. Although the dye is used for chemical sensing, the particle's magnetic content allows it to be manipulated under an applied magnetic field. As a demonstration of proof-of-concept, we chose to study the process of phagocytosis. During this process, a pathogen is internalized by immune cells (e.g., macrophages, neutrophils, and dendritic cells) in an organelle called the phagosome (10). This is followed by phagosomal maturation, during which the phagosome acidifies and the pH drops from near neutral to ~4.5–5. As a result of the acidic and hydrolase-rich environment of the matured phagosome, the pathogen is degraded and eliminated. During this process, the phagosome becomes attached to the cytoskeletal network and is transported in a centripetal fashion from the cell periphery toward the nucleus (11). This process leads to substantial reorganization of the cytoskeleton (12,13). Although the centripetal motion has been observed and recorded a number of times in the past (11,14), the driving force behind this movement is still not understood. It has been widely expected that this movement is caused to better facilitate phagosomal-endosomal fusion, owing to a higher concentration of endosomes near the cell center than at the cell periphery. The method presented here allows us not only to track the acidification of the phagosome in time but also to simultaneously observe cytoskeletal reorganization by measuring the local mechanical properties of the cells. The strength and novelty of this method lie in its ability to measure spatially resolved local intracellular chemical and micromechanical properties simultaneously. Interestingly, because this method allows spatial manipulation of the magnetic phagosomes, it also allows us to manipulate the intracellular location of the phagosome. Using magnetic tweezers, one can apply an opposing force on the magnetic phagosome, thereby completely stalling its inward motion and preventing its transport to the perinuclear region. As an extension to our method, we also present experimental results with regard to how preventing centripetal phagosomal motion affects the acidification kinetics.

The method as demonstrated here obviously is not limited to the study of phagocytosis. We believe it may find wide application in the field of cellular biophysics. Specific applications could include mechanochemical signaling pathways (e.g., the JNK pathway) and diseased cells (e.g., the altered mechanical properties of cancer cells (15) and those due to intracellular protein aggregation, as in Parkinson's disease and Alzheimer's disease).

THEORY

Passive microrheology

In the absence of an external force, the motion of a tracer particle in a liquid is chiefly governed by thermal fluctuations in the medium causing Brownian motion of the particle. The trajectory of the particle can be used to measure the micromechanical properties of the environment of the particle. This is referred to as passive microrheology. In the case of diffusion, the mean-square displacement (MSD) of the particle trajectory in combination with directed motion is given by

$$MSD = A^2 + 4D\Delta t + v^2\Delta t^2, \quad (1)$$

where D is the diffusion coefficient (m^2/s), v is the directed velocity of the particle caused by active processes of the cell (m/s), and A is the offset (m) due to localization inaccuracy, and Δt is the time interval. In general, the motion of a particle can also show confinement to a region of limited size. However, in the experiments shown in this work, we confirmed that at the time intervals used for fitting (0.4 s), the MSD did show directed motion and did not show any confinement, justifying the use of Eq. 1 to obtain the diffusion coefficient. From this value and the Einstein-Stokes relation ($\eta = k_B T/6\pi \cdot D \cdot r$), we can calculate the viscosity η of the environment, where r is the radius of the particle, k_B is Boltzmann's constant, and T is the temperature. It should be noted here that, as discussed in the Introduction, the diffusion coefficient as obtained by applying Eq. 1 might be strongly overestimated due to cell-induced active (but random) motion of the particle (3).

Active microrheology

An analytical model called the Voigt-Maxwell model can describe the displacement of a particle in a viscoelastic medium in response to an external force. It was previously

shown that this model works well for describing particle displacements in response to active forces inside the cytoplasm of a living cell (16). The model consists, in series, of a viscoelastic body (a dashpot characterized by damping coefficient γ_1 in parallel with a spring of spring constant k) with a dashpot characterized by damping coefficient γ_0 (9) (see also Fig. 1 *c*, *inset*). As a result of an external force, a particle placed in a viscoelastic medium shows a time-dependent response given by

$$\frac{x(t)}{F_{mag}} = \frac{1}{k}\left(1 - e^{-\frac{t}{\tau}}\right) + \frac{t}{\gamma_0} \text{ with } \tau = \frac{\gamma_1}{k}, \tag{2}$$

where at $t = 0$ the force F on the particle switches from $F = 0$ to $F = F_{mag}$, and the force on the particle is in the x-direction. The probe-independent bulk modulus (μ) and viscosity (η) of the viscoelastic medium can then be calculated as (17)

$$\eta = \frac{\gamma_0}{g};\ \mu = \frac{k}{g} \text{ wtih } g = 3\pi d_{bead}, \tag{3}$$

where d_{bead} is the probe diameter. It is assumed that the particle is placed in an isotropic environment.

MATERIALS AND METHODS

Experimental setup, particles, phagocytosis assay, and pH measurements

Experimental details regarding the setup, functionalization of magnetic pH-sensing particles, phagocytosis assay, and intracellular pH measurements can be found in the Supporting Material. In short, we used an in-house-built

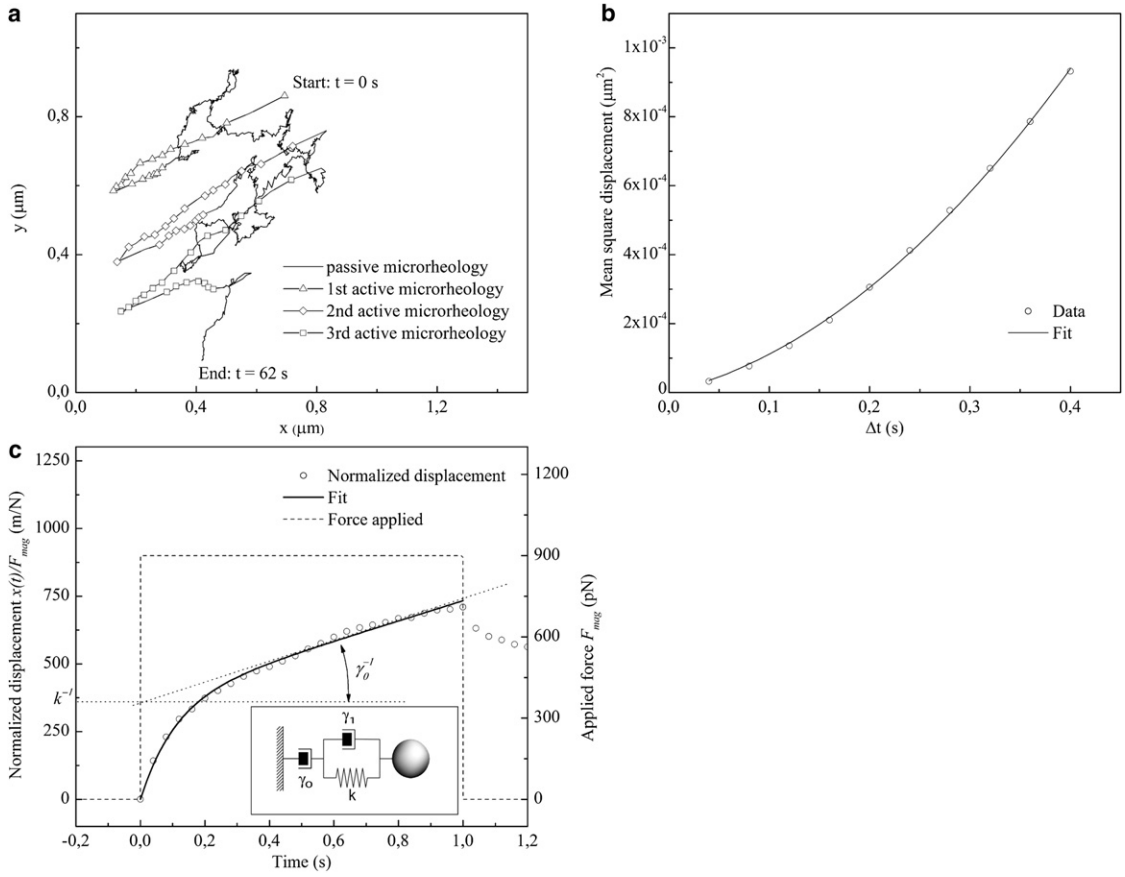

FIGURE 1 (*a*) Actual trajectory of a magnetic particle internalized by a cell over a duration of 62 s. A magnetic pulse was applied every 30 s for a duration of 1 s. The successive magnetic pulses are labeled with symbols. Passive microrheology is carried out over the nonlabeled part of the trajectory (when the force is switched off), and active microrheology is carried out in the labeled part of the track (when the force is switched on). The start and end of the particle trajectory are marked in the figure. (*b*) MSD of the particle trajectory where the particle carries out Brownian motion. The MSD data were fitted with Eq. 1 (*solid curve*) to determine the diffusion coefficient. The diffusion coefficient calculated from the fit was found to be 1.74×10^{-4} $\mu m^2/s$. Only the first 10% of data points (0.4 s) were used for the fit. (*c*) Displacement response (*circles*), normalized by force, of a bead inside the macrophage cytoplasm as a result of the application of a 900 pN force step (*dashed line*) and a fit (*solid line*) to the Voigt-Maxwell model (Eq. 2). The fast elastic response followed by a slower viscous response can be clearly seen in the curve. The dotted lines indicate the slope of the viscous part of the curve, which is a measure of the damping coefficient γ_0 and the y-intercept, which is a measure of the spring constant k. Inset: Voigt-Maxwell model for a viscoelastic body. The model consists, in series, of a viscoelastic body (a dashpot characterized by damping coefficient γ_1 in parallel with a spring of spring constant k) with a dashpot characterized by damping coefficient γ_0.

optical setup for simultaneous bright-field (for particle tracking) and fluorescence (for phagosomal pH measurement) imaging. Magnetic pH sensing particles were fabricated by functionalizing Dynal M270-particles (Invitrogen) with the pH-sensitive fluorophore SNARF-4f (Invitrogen) and opsonized with human IgG (18), referred to as M270-SNARF particles. RAW264.7 cells were used for all experiments.

Particle tracking, simultaneous active and passive microrheology with pH sensing, and data analysis

For details regarding the particle tracking, microrheology, and data analysis performed in this work, see the Supporting Material. In short, macrophage cells were allowed to internalize M270-SNARF beads. The position of the internalized bead was determined from bright-field images with an accuracy of ~8 nm using custom-written software. Active microrheology was performed by applying a magnetic force pulse for a duration of 1 s every 30 s. Particle motion obtained in between the magnetic force pulses was used for passive microrheology analysis (using Eq. 1). The data obtained during active microrheology were analyzed using Eqs. 2 and 3. In parallel, pH measurements were obtained. The resulting pH versus time curve was fitted with a sigmoidal function (19) to extract various parameters, including the initial pH (pre-acidification, pH_i), rate of acidification (pH_{rate}), and final pH (post-acidification, pH_f; see also Eq. S1). The time of onset of acidification (t_i) and time-point of end of acidification (t_f) were also determined (Eq. S2).

RESULTS

To simultaneously measure chemical and micromechanical properties, we simultaneously imaged the magnetic particle that was being phagocytosed by macrophage cells in bright field (to obtain the mechanical properties) and fluorescence (for ratiometric pH measurements). Here, we describe the microrheology measurements and distinguish between the active and passive approaches.

Passive microrheology

To illustrate the method used to obtain the micromechanical properties by both active and passive microrheology approaches, an example of a trajectory of a single phagocytosed particle over a duration of 62 s is presented in Fig. 1 *a*. These trajectories contain sections of actively induced movement due to magnetic force pulses. In between these pulses, the particle carries out Brownian diffusion combined with normal phagosomal transport. These stretches allow us to apply the principles of passive microrheology, as depicted in Fig. 1 *b*, which shows the MSD calculated during this part of the trajectory (for a window size of 4 s). The same figure also shows a fit of the data to Eq. 1 to extract the diffusion constant D. Clearly, the nonlinear nature of the MSD curve demonstrates that the particle motion is not purely diffusive but also includes directed motion. From the observed diffusion constant D, the average viscosity value was found to be $\eta = 0.95 \pm 0.24$ Pa·s. As a control to confirm that the viscosity measured by the passive method was not limited by the accuracy of the setup, we measured the Brownian motion of a similar probe particle in a material of known viscosity (silicone oil, $\eta = 22$ Pa·s at 300 K, which is an order of magnitude higher than our measured cellular viscosity). The measured viscosity of the silicone oil, 20 ± 3.4 Pa·s, is in close agreement with the known viscosity, confirming that the viscosity of the cell as determined by the passive method was not limited by the measuring technique. In addition, we tested whether the active pulling of the particle had any influence on the measured viscosity as determined with the passive method. No significant changes were observed in the viscosity before and after an active pull, and in addition, experiments in which no active pulls were performed showed similar values of viscosity (~1 Pa·s; see Fig. S5).

Active microrheology

We performed active microrheology by analyzing the response of the magnetic particle to the application of short magnetic force pulses. The response of the particle during such magnetic force steps is clearly visible in the observed trajectory (see Fig. 1 *a*). The sections of the trajectory during which magnetic force was turned on were used for active microrheology. Fig. 1 *c* shows the normalized displacement of the particle during a force pulse (amplitude 900 pN, duration 1 s). We calculate the displacement of the particle from the trajectory by calculating the movement of the particle in successive frames in the direction of the applied force. At short times ($t < \tau$), the particle experiences a fast elastic response followed by a slower viscous response. Curve fitting of the data using Eq. 2 confirms the applicability of the Voigt-Maxwell model. Note that the curve fit is only applied to the portion of particle response corresponding to when the force was switched on. Viscoelastic parameters such as the shear modulus and the viscosity of the phagosomal environment can be deduced from the fit. The average viscosity found using the active approach is $\eta = 1 \pm 0.09 \times 10^2$ Pa·s. This was measured as an average of 40 measurements carried out 30 s apart. We also determined whether the micromechanical properties as measured by active microrheology were dependent on the applied force. The normalized displacement curves of the particle displacement at different forces were largely seen to overlap with each other, indicating that decreasing or increasing the force does not significantly alter the determined viscoelastic parameters (see Fig. S6). It should be noted that the range of forces was limited, because for forces < 200 pN, the displacement of the particle is too small to allow for accurate analysis.

Combined microrheology and chemical sensing of the phagosome

Next, we combined the micromechanical measurements with chemical sensing. As a proof-of-principle, we applied

this approach to study phagosomal maturation. Fig. 2 shows a measurement of the time dependence of the viscoelastic parameters (as measured by active microrheology) as well as the pH of the phagosome from the time point of particle internalization up until the completion of acidification. The active pulling of the particle was performed such that the force was applied perpendicular to the normal phagosomal transport to minimize any influence of the measurement on the phagosomal maturation process. The normal inward transport of the phagosome did not seem to be affected, and the acidification kinetics obtained from experiments with active microrheology are similar to those observed in experiments without active microrheology. In the example shown in Fig. 2, we obtained an onset-of-acidification of ~4.5 min and an acidification rate of ~0.3 pH U/min, values that are consistent with those observed for nonperturbed transport (see Fig. 3 and Fig. S7). At time $t = 0$, the particle is internalized into a phagosome. Acidification starts at $t = 4.5$ min and is completed at $t = 12$ min. During acidification, the viscosity varies between a minimum value of $\eta_0 = 50$ Pa·s and a maximum value of $\eta_0 = 200$ Pa·s (i.e., by a factor of 4). The shear modulus μ varies between a minimum of $\mu = 45$ Pa and a maximum of $\mu = 315$ Pa, and thus varies by a factor of 7 over the duration of maturation. Although the observed changes in the micromechanical properties are significant, no apparent correlation with the changes in pH is observed. We repeated the experiment multiple times using different cells and particles, and all showed very similar behavior (data not shown). For comparison, the viscosity as determined by the passive microrheology method is also shown in Fig. 2. Here an average of $\eta_0 = 0.95 \pm 0.24$ Pa·s is observed. As with the active method, no clear apparent changes in viscosity are observed

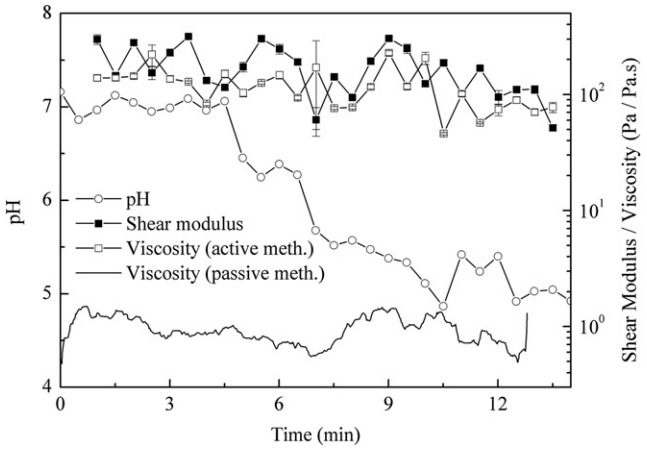

FIGURE 2 Evolution of shear modulus (*solid squares*) and viscosity (*open squares*) in the immediate vicinity of the phagosome measured with the active microrheology approach, and the pH of the phagosome (*open circles*) as a function of time during phagosome acidification. Viscosity measured with passive microrheology (*solid*) is also plotted. A clear difference in viscosity between the active and passive methods (of 2 orders of magnitude) is seen.

that can be correlated to changes in pH. The results shown above demonstrate the key aspects of the developed method. In the remainder of this work, we will discuss additional possible applications of this method in cellular biophysics.

Active manipulation of phagosome transport

In addition to the measurement of micromechanical properties, magnetic tweezers allow active manipulation of cellular processes. We exploited this aspect to study the relationship between the perinuclear localization of the phagosome and its maturation, by preventing the centripetal transport of the phagosomes. To that end, we applied magnetic forces on a phagosome to prevent its intracellular transport. Before applying a magnetic force, it is essential to ensure that the particle has actually been completely internalized. For this purpose, we used the GFP-tagged polycationic probe K-myr, a K-Ras-derived peptide that binds to anionic lipids (20). Upon transfection and subsequent expression, K-myr-GFP is localized on the plasma membrane of the macrophage cells. Phagocytosis involves particle binding on the macrophage cells, followed by formation of a phagocytic cup. Using the K-myr-GFP membrane marker, we were able to observe the formation and closing of this phagocytic cup, with the time-point of closing defined as $t = 0$ (or t_0; see Fig. S8 and Movie S1).

As described above, we applied an external magnetic force to prevent phagosomal centripetal transport. Fig. 3 shows the effect of applying an external force on the location of a particle internalized by a macrophage cell. The figure shows time-lapse images at the time of internalization t_0 and at $t = 10$ min in the absence (*A* and *B*) and presence (*C* and *D*) of force. In the absence of force (the control experiment), the phagosome can be clearly seen to move from the plasma membrane toward the perinuclear region between t_0 and $t = 10$ min (Fig. 3, *a* and *b*, and Movie S2). However, in the presence of force, the phagosomal transport is hindered and the phagosome remains close to the plasma membrane even after 10 min of internalization (Fig. 3, *c* and *d*, and Movie S3). Here, the force is switched on immediately after t_0. The direction of the force is such that it opposes the centripetal transport. The amplitude of the force is modified manually during the experiment such that the force is high enough to prevent cellular transport of the phagosome, but low enough to prevent rupture of the cell. From Fig. 3 *d* it is clear that the phagosome-to-cell-body distance changes slightly over time. This is not caused directly by pulling the phagosome away from the cell body, but is a result of the response of the cell to the manipulation of the phagosome. During the course of the experiment, while keeping the phagosome close to the cell periphery, we noticed that the cells had a tendency to move and extend in the direction of the phagosome. We compensated for this movement of the cell by manipulating the phagosome back to the cell periphery.

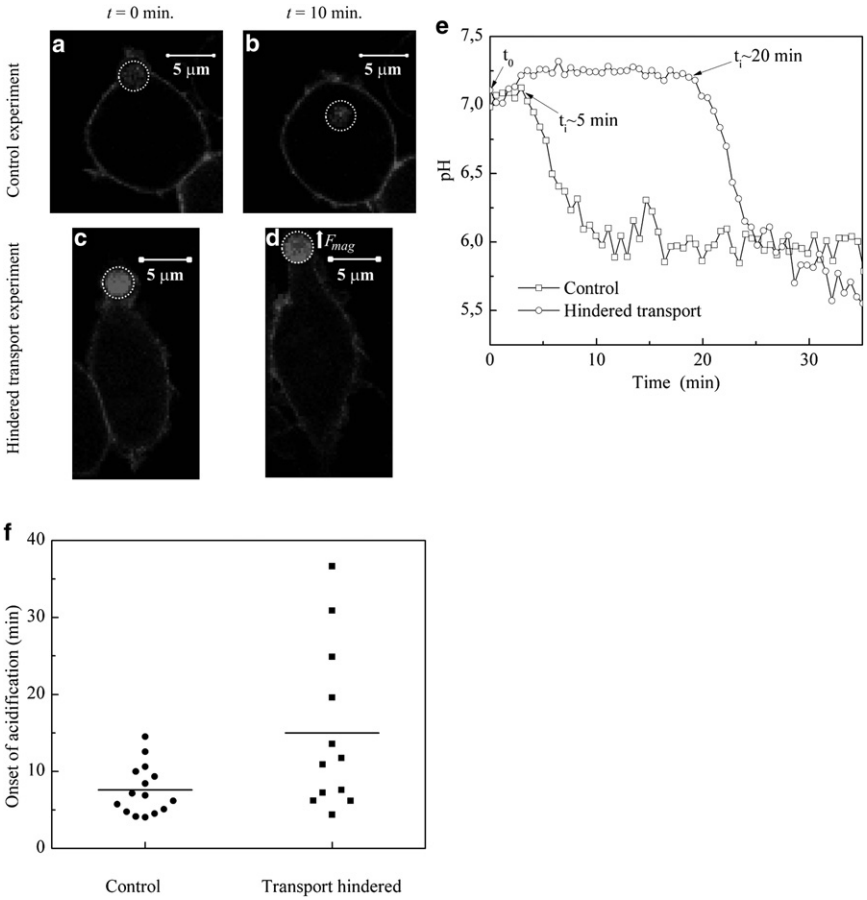

FIGURE 3 (*a–d*) Location of a particle internalized (*dotted circle*) by a RAW 264.7 macrophage. Time-lapse images show the location of the phagosome in the absence and presence of an external force. The two frames are 10 min apart. Scale bar: 5 μm. (*a* and *b*) Normal transport of a phagosome from the plasma membrane toward the perinuclear region. (*c* and *d*) In the presence of an external force, the phagosome stays at the plasma membrane for the entire duration of experiment. The white arrow shows the direction of applied force. The two frames are 10 min apart. (*e*) An example of two individual pH curves, one each for normal transport (*squares*) and hindered phagosomal transport (*circles*). The particles were internalized at $t = 0$ min (or t_0). Onset of acidification for the phagosome with hindered transport is delayed by 20 min, compared with 5 min for the phagosome with normal centripetal transport. (*f*) Distribution of the time of onset of acidification for the two conditions: control experiment with normal phagosomal transport (*circles*, $n = 15$) and hindered phagosomal transport due to magnetic force (*squares*, $n = 12$). The flat line in the curves indicates the averages for the two conditions.

To monitor the effect of the hindered phagosomal transport on maturation, we measured the pH of the phagosome during the entire experiment. We fitted the pH versus time data using Eq. S1 to determine the time of onset of acidification (t_i) and the rate of acidification (pH_{rate}; see Supporting Material). Fig. 3 *e* shows an example of acidification profiles of two phagosomes, one in each condition. On average, the phagosomes acidified at a rate of 0.5 ± 0.09 pH U/min in both the control experiment and the hindered-transport experiment. This suggests that the rate of phagosomal acidification was independent of whether the phagosome moved to the perinuclear region or not. We then looked at the time of onset of acidification (t_i). As can be seen in the acidification curves, the onset of acidification was considerably delayed in the case of hindered transport of the phagosome. Fig. 3 *f* shows a plot with the times of onset of acidification for individual phagosomes. Results are presented for 15 different phagosomes/cells for the control experiment and 12 in the presence of external force. In control experiments, all phagosomes began to acidify between 5 and 15 min after internalization, with a mean $\overline{t_i} = 7.5$ min. However, when phagosomal transport was hindered as a result of application of external force by magnetic tweezers, we found a mean $\overline{t_i} = 15$ min. The observed spread in the times of onset is quite large; ~70% of the phagosomes initiated acidification at t_i in the range of 5–15 min, and 30% of phagosomes showed a delayed acidification, with $t_i > 15$ min. Thus, a clear delay in the onset of acidification, with some phagosomes even taking as long as 38 min to begin acidification, is observed when transport of the phagosome is hindered. The observed means are significantly different as determined by a Student's *t*-test ($p < 0.05$). We did not notice any direct relation between the extent of phagosome displacement and the observed onset times. The results obtained by manipulating the phagosomes indicate that phagosomal acidification is an all-or-nothing process. Preventing centripetal motion delays the beginning of acidification, but once acidification starts, it occurs at a rate that is independent of the transport history of the phagosome.

Cyclic acidification events

While performing the manipulation experiments, we came across an unexpected phenomenon. In a normal phagosomal acidification event, the phagosome begins to acidify from an initial pH (pH_i) to a final post-acidification pH (pH_f). When pH_f is reached, an equilibrium is achieved and the phagosomal pH remains at pH_f with no further major changes in acidification. However, in our experiments, we at times

observed multiple acidifications for a single phagosome, i.e., the pH of an acidified phagosome rose back to near-neutral pH, followed by reacidification until it reached the low pH again. This cycle of acidification and deacidification continued repeatedly. Fig. 4 shows an example of one such acidification pulse. As can be seen in the figure, the phagosome begins to acidify from an initial pH of 7.0 at t = ~17 min and finally reaches a pH of 5.0. At t = 28 min, the pH of the phagosome once again reaches back to near neutral. In all, three such acidification pulses were observed for this particular phagosome during the duration of the experiment. Although the effect of multiple acidifications was observed in both the control and hindered-transport experiments, it was seen more often in the latter. In the presence of the external force, ~15% of acidified phagosomes showed this phenomenon. In comparison, only ~5% of phagosomes showed this effect in the case of phagosomes with normal centripetal transport. These numbers are based on ~50 recorded experiments for each condition. The phagosomes with hindered transport also showed a higher frequency of these pulses. On average, phagosomes with hindered transport acidified once every 3.2 ± 0.4 min as compared with once every 7.1 ± 1.1 min for phagosomes in the control experiment. The biological significance of this effect is not clear at this time. However, as demonstrated clearly by these experiments, the biophysical tools presented here provide a powerful means to influence biological processes and thus obtain deeper insight into these processes.

DISCUSSION

We have demonstrated a novel (to our knowledge) approach that uses functionalized magnetic particles to enable simultaneous local measurement of intracellular chemical (in this case, the local pH) and micromechanical properties. As a proof-of-concept, we applied this approach to study the process of phagocytosis. Using functionalized magnetic particles, we successfully probed the mechanical properties of the phagosomal environment while at the same time we measured the decrease in pH inside the phagosome.

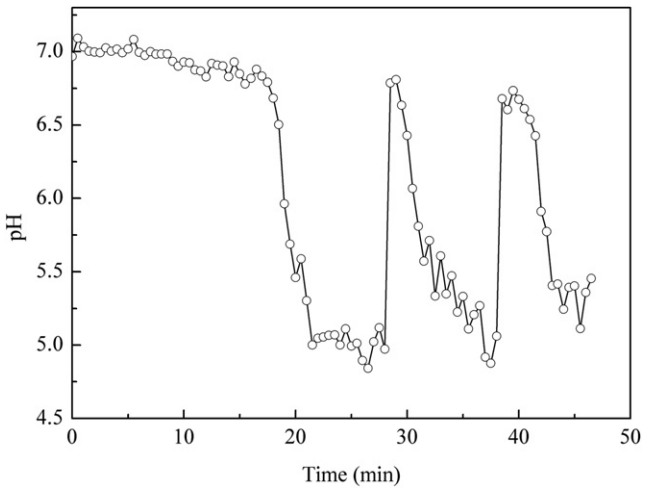

FIGURE 4 Repeated acidification cycles of a phagosome with hindered transport.

We measured viscoelastic properties by both active and passive microrheology using the same probe. The viscosity obtained using the passive method (~1 Pa·s) is ~2 orders of magnitude lower than that measured by the active method (~100 Pa·s). We confirmed that this was not limited by the experimental method. We hypothesize that the apparent lower viscosity measured by the passive method is caused by contamination of the particle Brownian motion due, for example, to active cellular motions such as motor trafficking, cytoskeleton remodeling, and cell crawling. If these active motions are random in nature on the timescale of the experiment (0.4 s), this will give rise to an increased slope of the calculated MSD curves, and as such result in a higher diffusion and hence a lower derived viscosity. It should be noted here that the validity of passive microrheology techniques in live cells is highly debated (21). Application of the Stokes-Einstein relation assumes that the particle motion is governed purely by thermal fluctuation. However, the presence of various active processes in the intracellular environment gives rise to an apparent enhanced diffusion that results in a lower viscosity of the cellular environment. Hoffman et al. (3) measured a change in viscoelastic properties as a result of ATP depletion, confirming the contribution of active processes to the apparent enhanced diffusion of the probe. In addition, lysosome fusion with the phagosome is likely to increase the volume of the phagosome by further adding lysosomal content that presumably has a low viscosity. Because the passive method measures more locally than the active method, this could (partially) explain our observations, although we did not observe any changes in viscosity during the course of the experiment, as one might expect in this case. Our comparison of the two approaches clearly shows the advantages of the active method over the passive method: it is faster because particle displacement by a 1-s-long pulse is sufficient to measure the viscoelastic parameters, and it is independent of active intracellular processes. Although the passive method does not seem to be useful for determining the viscoelastic properties of a cell in the case of phagosomes, the combination of both passive and active methods may still be very useful for a number of reasons. First, phagosomes may be more prone to active motion of the cell because they are coupled to the cytoskeleton by molecular motors. The use of naked particles (e.g., as introduced by microinjection) might yield different results. Further, the active method is not sensitive to cell-induced particle movements, whereas the passive method includes both Brownian and cell-induced movements. A comparison of data obtained by both methods can yield information about elastic and viscous properties as well as active cellular processes. Nevertheless, in the

remainder of the discussion, we will consider only the parameters measured by active microrheology.

Feneberg et al. (22) reported elasticity values ranging from 10 to 100 Pa and viscosity ranging from 10 to 350 Pa·s in *Dictyostelium* cells, whereas Bausch et al. (23) reported elasticity values of 20–735 Pa and viscosity values of ~200 Pa·s in fibroblast cells. A micropipette aspiration study showed an intracellular viscosity of 930 Pa·s for J774 macrophages at room temperature, which is ~10 times our measured values (24). These values are actually quite comparable if we take into account the different techniques and temperatures used. The temperature dependence of the cytoplasmic viscosity of granulocytes was reported in an earlier study (25). All reported values are of the same order of magnitude as found in our experiments ($\mu = 45$–315 Pa; $\eta = 50$–200 Pa·s). It was previously reported that the shear modulus over a single fibroblast cell can vary by a factor of 2, but the viscosity varies by much less (23). We observed similar trends in our experiments; however, the magnitude of variation was higher in our results. In our experiments, the shear modulus over a single cell varied by as much as a factor of 7 over the duration of phagosomal maturation. However, one should keep in mind that these variations can be due either to variations over time or to variations in position within the cell. It is not possible to distinguish one from the other in the current experiment. Moreover, we found no correlation between the observed fluctuations in the viscoelastic properties and phagosomal maturation. During the course of the experiment, changes in the micromechanics seemed to be random. A comparison of traces acquired from different cells also did not yield any observable trends. In addition, no correlation was observed between the variation in shear modulus and the viscosity.

The magnetic forces applied to the particle seemed to be high enough to cause intracellular displacement of the magnetic particle containing the phagosome. This allowed us to prevent the intracellular transport of the phagosome by applying a magnetic force opposing the direction of transport. One of the major advantages of using our method compared with more commonly used biochemical methods, such as cytoskeleton-disrupting drugs, is that it does not affect any other cellular process. Disrupting the cytoskeleton or knocking down other proteins can lead to other, unwanted cellular effects because these elements are involved in many other cellular processes.

V-ATPase, a proton pump that consumes ATP to pump hydrogen ions through the phagosomal membrane is the main actor in the acidification process. The origin of V-ATPases has been widely debated. Some investigators proposed that it is directly recruited from the plasma membrane during phagosome formation (26), whereas others suggested that V-ATPases are acquired by phagosomal fusion with lysosomes (27). It is widely accepted that the phagosomal motion toward the perinuclear region is likely relevant for promoting phagosome-lysosome fusion, as suggested by the observation that the concentration of lysosomes is larger near the nucleus than at the cell periphery (28). The results of our experiments show that preventing the inward phagosome transport delays the onset of phagosomal acidification. There was a 100% increase in the time taken for the beginning of acidification, up from the average of 7.5 min in the control to 15 min in the case of hindered phagosomal transport. The phagosomes with hindered centripetal transport showed a wider spread in onset of acidification than those in the control experiment. Interestingly, this delay in the beginning of acidification did not affect the rate of acidification, that is, once the acidification began, the acidification occurred at the same rate independently of whether the phagosome moved to the perinuclear region or not. It should be noted that we observed a large standard deviation in the measured rate of acidification (~0.6 pH U/min) in the different phagosomes for both normal and hindered phagosomal transport. This is in line with the previously reported large phagosome-to-phagosome variation in phagosomal maturation behavior (29).

Upon internalization, the phagosome does not immediately start to acidify, and there exists a lag between internalization and onset of acidification. It was previously suggested that full-scale acidification is initially prevented by leakage through the phagosomal membrane compensating for the pumped protons (30). Acidification fully sets in once the leakage slowly begins to be plugged, until a new equilibrium is established at a lower pH. It is also possible that a minimum threshold in the number of active proton pumps needs to be achieved to overcome the leakage and initiate full-scale acidification. We hypothesize that hindering phagosomal transport delays the time required to reach the threshold of accumulated proton pumps. Once the threshold is reached, acidification occurs at the same rate as in normal phagosomal transport, which would be in line with our observations. However, more experiments examining the molecular consequences of hindering phagosomal transport need to be carried out before this hypothesis can be conclusively established. Observing the recruitment of specific maturation markers (e.g., Rab5, Rab7, and Lamp2) will also shed light on the link between transport and phagosomal maturation as a whole.

The hybrid magnetic particle manipulation and sensing method can be widely applied in cellular biophysics. The method is flexible, in that depending on the application, specific magnetic particles can be selected in combination with appropriate chemical sensors. The pH-sensing dye on the particle can easily be replaced with various other sensors to measure other properties (e.g., fluorescence resonance energy transform sensors to measure protease and lipase activities) (31). In addition, it is important to select the particle size carefully. Here, we used particle diameters of 2.8 μm; however, particles with smaller diameter can also be used. Using smaller particles as opposed to larger particles provides multiple advantages, such as higher spatial

resolution in measuring chemical properties, less structural interference caused to the immediate cellular environment, and larger Brownian fluctuations, which allow measurements of even higher viscosities. We have demonstrated that with the use of our magnetic-tweezers setup, it is possible to apply forces as high as 4 nN at a distance of 25 μm. This corresponds to a high magnetic flux gradient of ~30 kT/m. This approach can easily be applied to particles of smaller diameter. Of course, the force applied on smaller particles will be much smaller owing to their lower magnetization. Using the same setup, the force applied on 1 μm (Dynal MyOne) and 350 nm particles would be ~400 pN and ~40 pN, respectively. Experiments have shown that it is possible to manipulate particles down to 350 nm in live cells (16).

In this work, we have reported the novel (to our knowledge) observation of a phagosome undergoing repeated cycles of acidification. The phagosomal pH alternates between cycles of acidic and near-neutral pH. Interestingly, the effect was observed three times more often in phagosomes whose centripetal transport was hindered than in those with normal centripetal transport. The cause of these repeated acidification pulses is unknown at this time. The phagosomes in hindered-transport experiments also showed a higher frequency of acidification pulsing (once every 3.2 $\pm$ 0.4 min as compared with once every 7.1 $\pm$ 1.1 min for the control experiment). As discussed above, we believe that hindering phagosomal transport may delay the accumulation of V-ATPase pumps, in turn delaying the equilibrium state in which the phagosome acidifies unhindered by proton leakage. It is possible that the phagosomes showing the acidification pulses have a V-ATPase concentration close to (but not very much higher than) the critical concentration required to compensate for the leakage. As a result, a stable equilibrium is not reached, and only a delicate equilibrium between leakage and pumping exists that can be disturbed as a result of the slight change in V-ATPase pump concentration on the phagosome membrane. Therefore, although the acidification is completed in every cycle, the proton leakage quickly takes precedence over pumping and the phagosome pH goes back to neutral. However, more detailed experiments need to be conducted before this hypothesis can be established. Nevertheless, we believe that in the future this effect could be used as a tool to mimic pathogen-containing phagosomes that show inefficient/incomplete acidification.

CONCLUSIONS

In conclusion, we have presented a novel (to our knowledge) approach that uses magnetic tweezers to measure local intracellular chemical and micromechanical properties simultaneously. We demonstrated an application of this method by simultaneously measuring the acidification of a phagosome and the viscoelastic properties of the phagosomal environment. Additionally, we demonstrated the potential of this approach for manipulating specific cellular processes. We believe our approach could find wide application in cellular biophysics.

SUPPORTING MATERIAL

Materials and Methods, eight figures, a table, three movies, and references (32,33) are available at http://www.biophysj.org/biophysj/supplemental/S0006-3495(12)00666-2.

We thank Ben Joosten and Robert Molenaar for technical support, and Sergio Grinstein (Toronto, Ontario, Canada) for the generous gift of the K-myr-GFP plasmid.

S.S. is the recipient of a Marie Curie Research fellowship from the European Commission (Marie Curie Research Training Network IMMUNANOMAP contract number MRTN-CT-2006-035946). A.C. received a MEERVOUD subsidy and C.G.F. received the Spinoza Prize from The Netherlands Organisation for Scientific Research.

REFERENCES

1. Carafoli, E. 2002. Calcium signaling: a tale for all seasons. *Proc. Natl. Acad. Sci. USA.* 99:1115–1122.
2. Ketene, A. N., E. M. Schmelz, …, M. Agah. 2011. The effects of cancer progression on the viscoelasticity of ovarian cell cytoskeleton structures. *Nanomedicine.* 8:93–102.
3. Hoffman, B. D., G. Massiera, …, J. C. Crocker. 2006. The consensus mechanics of cultured mammalian cells. *Proc. Natl. Acad. Sci. USA.* 103:10259–10264.
4. Smith, B. A., B. Tolloczko, …, P. Grütter. 2005. Probing the viscoelastic behavior of cultured airway smooth muscle cells with atomic force microscopy: stiffening induced by contractile agonist. *Biophys. J.* 88:2994–3007.
5. Skibbens, R. V., and E. D. Salmon. 1997. Micromanipulation of chromosomes in mitotic vertebrate tissue cells: tension controls the state of kinetochore movement. *Exp. Cell Res.* 235:314–324.
6. Caspi, A., R. Granek, and M. Elbaum. 2002. Diffusion and directed motion in cellular transport. *Phys. Rev. E s.* 66:011916.
7. Möller, W., I. Nemoto, …, J. Heyder. 2000. Magnetic phagosome motion in J774A.1 macrophages: influence of cytoskeletal drugs. *Biophys. J.* 79:720–730.
8. Bausch, A. R., F. Ziemann, …, E. Sackmann. 1998. Local measurements of viscoelastic parameters of adherent cell surfaces by magnetic bead microrheometry. *Biophys. J.* 75:2038–2049.
9. de Vries, A. H., B. E. Krenn, …, J. S. Kanger. 2007. Direct observation of nanomechanical properties of chromatin in living cells. *Nano Lett.* 7:1424–1427.
10. Haas, A. 2007. The phagosome: compartment with a license to kill. *Traffic.* 8:311–330.
11. Harrison, R. E., C. Bucci, …, S. Grinstein. 2003. Phagosomes fuse with late endosomes and/or lysosomes by extension of membrane protrusions along microtubules: role of Rab7 and RILP. *Mol. Cell. Biol.* 23:6494–6506.
12. Liebl, D., and G. Griffiths. 2009. Transient assembly of F-actin by phagosomes delays phagosome fusion with lysosomes in cargo-overloaded macrophages. *J. Cell Sci.* 122:2935–2945.
13. May, R. C., and L. M. Machesky. 2001. Phagocytosis and the actin cytoskeleton. *J. Cell Sci.* 114:1061–1077.
14. Al-Haddad, A., M. A. Shonn, …, S. A. Kuznetsov. 2001. Myosin Va bound to phagosomes binds to F-actin and delays microtubule-dependent motility. *Mol. Biol. Cell.* 12:2742–2755.

15. Wirtz, D. 2009. Particle-tracking microrheology of living cells: principles and applications. *Annu. Rev. Biophys.* 38:301–326.

16. de Vries, A. H., B. E. Krenn, …, J. S. Kanger. 2005. Micro magnetic tweezers for nanomanipulation inside live cells. *Biophys. J.* 88:2137–2144.

17. Ziemann, F., J. Rädler, and E. Sackmann. 1994. Local measurements of viscoelastic moduli of entangled actin networks using an oscillating magnetic bead micro-rheometer. *Biophys. J.* 66:2210–2216.

18. Shekhar, S., A. Klaver, …, J. S. Kanger. 2010. Spatially resolved local intracellular chemical sensing using magnetic particles. *Sens. Actuators B Chem.* 148:531–538.

19. Blanchette, C. D., Y. H. Woo, …, A. L. Hiddessen. 2009. Decoupling internalization, acidification and phagosomal-endosomal/lysosomal fusion during phagocytosis of InlA coated beads in epithelial cells. *PLoS ONE.* 4:e6056.

20. Yeung, T., M. Terebiznik, …, S. Grinstein. 2006. Receptor activation alters inner surface potential during phagocytosis. *Science.* 313: 347–351.

21. Kasza, K. E., A. C. Rowat, …, D. A. Weitz. 2007. The cell as a material. *Curr. Opin. Cell Biol.* 19:101–107.

22. Feneberg, W., M. Westphal, and E. Sackmann. 2001. *Dictyostelium* cells' cytoplasm as an active viscoplastic body. *Eur. Biophys. J.* 30:284–294.

23. Bausch, A. R., W. Möller, and E. Sackmann. 1999. Measurement of local viscoelasticity and forces in living cells by magnetic tweezers. *Biophys. J.* 76:573–579.

24. Lam, J., M. Herant, …, V. Heinrich. 2009. Baseline mechanical characterization of J774 macrophages. *Biophys. J.* 96:248–254.

25. Evans, E., and A. Yeung. 1989. Apparent viscosity and cortical tension of blood granulocytes determined by micropipet aspiration. *Biophys. J.* 56:151–160.

26. Gluck, S. 1992. V-ATPases of the plasma membrane. *J. Exp. Biol.* 172:29–37.

27. Sun-Wada, G. H., H. Tabata, …, Y. Wada. 2009. Direct recruitment of H^+-ATPase from lysosomes for phagosomal acidification. *J. Cell Sci.* 122:2504–2513.

28. Falcón-Pérez, J. M., R. Nazarian, …, E. C. Dell'Angelica. 2005. Distribution and dynamics of Lamp1-containing endocytic organelles in fibroblasts deficient in BLOC-3. *J. Cell Sci.* 118:5243–5255.

29. Griffiths, G. 2004. On phagosome individuality and membrane signalling networks. *Trends Cell Biol.* 14:343–351.

30. Steinberg, B. E., K. K. Huynh, and S. Grinstein. 2007. Phagosomal acidification: measurement, manipulation and functional consequences. *Biochem. Soc. Trans.* 35:1083–1087.

31. Yates, R. M., A. Hermetter, and D. G. Russell. 2005. The kinetics of phagosome maturation as a function of phagosome/lysosome fusion and acquisition of hydrolytic activity. *Traffic.* 6:413–420.

32. Hosu, B. G., K. Jakab, …, G. Forgacs. 2003. Magnetic tweezers for intracellular applications. *Rev. Sci. Instrum.* 74:4158–4163.

33. Dawson, R. M. C., D. C. Elliot, …, K. M. Jones. 1986. Data for Biochemical Research. Oxford Science Publications, Oxford/ New York.